J|A|C|S
ARTICLES
Published on Web 12/15/2001

An Ab Initio Study of Amide Proton Shift Tensor Dependence on Local Protein Structure

Yugal Sharma, Oh Young Kwon,[§] Bernie Brooks, and Nico Tjandra*

Contribution from the Laboratory of Biophysical Chemistry, Building 50, National Heart, Lung, and Blood Institute, National Institutes of Health, Bethesda, Maryland 20892-8013

Received August 16, 2001. Revised Manuscript Received October 23, 2001

Abstract: Ab initio shielding tensor calculations were carried out on residues in human ubiquitin. Reported experimental data on isotropic and anisotropic components of the amide proton chemical shifts were used as benchmarks to test the validity of the chosen basis sets as well as methods in structure optimization and shielding calculations. The best agreement with the experimental values was observed when the 6-311**G and 6-311++G(2d,2p) basis sets were used to optimize the structure and to calculate the shielding tensor, respectively. The same method was employed in subsequent model calculations to characterize the dependence of amide proton shielding to the local structure. Both the isotropic and the anisotropic components of the symmetric tensor were found to depend very strongly on the hydrogen bond length. A weaker dependence can also be observed for the hydrogen bond angle. Antisymmetric tensor elements were found to be relatively small. This study permits separation of various local structure contributions to the amide proton shielding tensor that complements scarce experimental data.

Introduction

A proton chemical shift is the primary nuclear magnetic resonance (NMR) marker in studies of biomolecules. In biomolecular structure determination, distance information is derived mostly from dipolar interactions between pairs of protons.[1] The ability to observe all of the proton shifts in the protein, from which the dipolar interactions can be probed, determines the overall quality of the final structure. Direct application of chemical shifts in solution NMR for structure determination has seen some varying success. Carbon chemical shifts are used routinely in structure refinement to improve quality of backbone conformation.[2] In contrast, incorporation of the proton isotropic shift in structure determination,[3] which is largely based on the work of Williamson and Asakura,[4] is not very commonly used. The proton isotropic shift is broken down into several empirical shielding effects that can be calculated from a given geometry. This approach is generally applicable to aliphatic protons. However amide protons can be susceptible to additional local structural effects, thus rendering the use of its shielding information as not straightforward. The use of shielding information in protein structure determination is limited to the level of our understanding of various structural contributions to the shielding tensor.

Several empirical studies of isotropic H^N shifts from a NMR database suggested that they depend on the secondary structure of the protein.[5−9] Furthermore, it is also well known that hydrogen bonds will influence the isotropic H^N shift considerably. A recent study of H^N chemical shift anisotropy,[10] which was based on its cross correlation to the H^N-N dipolar interaction, suggested that it also depended on the hydrogen bond length. However, a similar study[11,12] concluded that the H^N chemical shift anisotropy (CSA) depends on the secondary structure, thus the backbone angles φ and ψ, and not necessarily the hydrogen bond strengths. These contradicting results cannot be resolved easily on the basis of the experimental data alone, since it is still possible that both the secondary structure and the hydrogen bond lengths might contribute in varying degrees to the CSA values. Note, however, that these measurements of H^N shielding tensor in solution are limited to just a few of its components, which are the isotropic value and the projection of the tensor along the N−H bond. In solid-state NMR, the measurement of the full chemical shift tensor is possible; however, measuring it for protons is still a challenging problem. The broad application of the recently developed solid-state NMR method for the study of oriented membrane proteins (PISEMA)[13,14] relies on an accurate knowledge of the H^N CSA tensor

* To whom correspondence should be addressed. Phone: (301) 402-3029. Fax: (301) 402-3405. E-mail: nico@helix.nih.gov.

§ Current address: Chemon Inc, BMP, #464-5, Jung-ri, Kusong-myon, Yongin City, Keongki-do, Korea.

(1) Wüthrich, K. *NMR of Proteins and Nucleic Acids*; Wiley: New York, 1986.
(2) Kuszewski, J.; Qin, J.; Gronenborn, A. M.; Clore, G. M. *J. Magn. Reson., Ser. B* **1995**, *106*, 92−96.
(3) Kuszewski, J.; Gronenborn, A. M.; Clore, G. M. *J. Magn. Reson., Ser. B* **1995**, *107*, 293−297.
(4) Williamson, M. P.; Asakura, T. *J. Magn. Reson., Ser. B* **1993**, *101*, 63−71.
(5) Wishart, D. S.; Sykes, B. D.; Richards, F. M. *J. Mol. Biol.* **1991**, *222*, 541−546.
(6) Wishart, D. S.; Sykes, B. D.; Richards, F. M. *Biochemistry* **1992**, *31*, 1647−1651.
(7) Wishart, D. S.; Sykes, B. D. *Methods Enzymol.* **1994**, *239*, 363−392.
(8) Williamson, M. P. *Biopolymers* **1990**, *29*, 1423−1431.
(9) Ösapay, K.; Case, D. A. *J. Am. Chem. Soc.* **1991**, *113*, 9436−9444.
(10) Tjandra, N.; Bax, A. *J. Am. Chem. Soc.* **1997**, *119*, 8076−8082.
(11) Tessari, M.; Mulder, A. A. F.; Boelens, R.; Vuister, G. W. *J. Magn. Reson.* **1997**, *127*, 128−133.
(12) Tessari, M.; Vis, H.; Boelens, R.; Kaptein, R.; Vuister, G. W. *J. Am. Chem. Soc.* **1997**, *119*, 8985−8990.

10.1021/ja016859d CCC: $22.00

and its dependence on local geometry.[15] Recently the average shielding tensors for H^N, $^{13}C'$, and ^{15}N have been determined for human ubiquitin that was aligned in a magnetic field by the addition of dilute liquid crystalline medium.[16] The non-residue-specific H^N shielding tensor obtained did not reveal any dependence on local structure. So far it is obvious that the separation of various contributions to the shielding tensor is not possible when one only relies on the available experimental data.

In the past few years the ab initio calculation of shielding tensors has improved dramatically due to advancement in methodology and computational hardware. Nevertheless the proton chemical shielding calculation is still challenging due to the need for a dense basis set as well as for a highly optimized structure to yield acceptable accuracy. Unfortunately this is the only approach that allows one to study individual structural contribution to the shielding tensor in detail. In solution NMR, most calculated shielding tensors can only be compared to the experimentally obtained isotropic shifts due to the lack of other available data. This leaves the anisotropy as well as the direction of the tensor to be unchecked. In this study, the availability of the isotropic and the anisotropic shifts as well as the average tensor provides excellent means of validating the tensor calculation protocol. Only when the calculated tensor reproduces the experimental data can one use the same protocol to carry out the model calculation to evaluate the dependence of the shielding tensor on individual structural features.

Materials and Methods

Experimental values for isotropic and anisotropic shifts were taken from solution NMR studies on human ubiquitin.[10] Ab initio studies were performed using Gaussian 98 (revision A.6) on individual residues in ubiquitin, using the X-ray coordinates as starting structures.[17] Hydrogens were added to the X-ray structure using the program XPLOR.[18] Only residues which are not solvent accessible were used in the calculation. Acetamide (AcAm) was included with each residue as a substitute for the peptide bond moiety and to represent the hydrogen bond acceptor. Previous studies have shown *N*-methylacetamide (MeAcAm) to be a good substitute for the peptide bond;[19,20] however, we found AcAm to give similar results (data not shown) and have used this molecule in subsequent calculations. The residue−AcAm pair was optimized using the 6-311**G basis set, keeping the backbone ϕ and ψ angles of each residue constant at its X-ray coordinates, along with hydrogen bond lengths and angles. Ala 28 of ubiquitin was chosen as a model for the single residue calculation. To study the dependence of shielding on hydrogen bond distance, the distance was varied from 1.5 to 3.2 Å while the hydrogen bond angle was kept fixed at the original X-ray value. Similarly while the hydrogen bond angle was varied from 70 to 180° to look at its effect on shielding, the distance was fixed to the original X-ray structure. Shielding tensor calculations were then performed on the optimized coordinates, using three different basis sets of increasing complexity for comparison. The resulting rank 2 CSA tensor (**T**) was separated into its symmetric ($\mathbf{T}^S$) and antisymmetric ($\mathbf{T}^A$) components. Analysis of the symmetric tensor yields the principal elements σ_{11}, σ_{22}, and σ_{33} as eigenvalues, along with the corresponding principal axes as eigenvectors. Figure 1 indicates the relative orientation of the H^N tensor components with respect to the peptide plane for a generic amide bond with the hydrogen bonding partner, AcAm. The isotropic shift (σ_{iso}) was calculated as $\mathrm{Tr}(\mathbf{T}^S)/3$. For direct comparison to NMR results, the CSA ($\sigma_{||}-\sigma_{\perp}$) was calculated as the $P_2(\cos\theta)$ projection of $\mathbf{T}^S$ onto the N−H bond, where θ is the angle between the N−H bond and the unique axis of the symmetric CSA tensor.

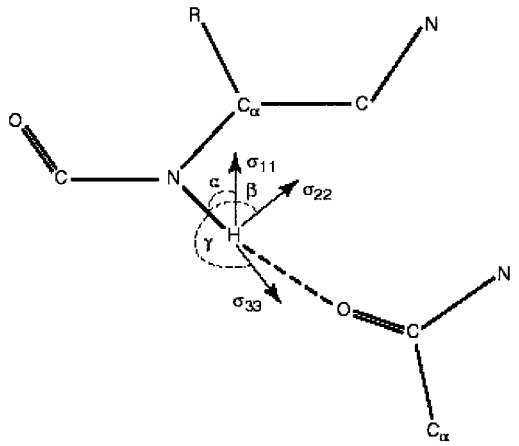

Figure 1. Representation of the molecular system used in the calculation and the average orientation of the principal axis of the shielding tensor in the molecular frame. The orientation of the H^N CSA tensor components with respect to the peptide plane is indicated. The least shielded σ_{11} axis is orthogonal to the peptide plane, σ_{22} is almost perpendicular to the N−H bond and in the peptide plane, whereas σ_{33} is nearly parallel to the N−H bond. Orientations are defined as the angle made between σ_{11} and the N−H bond (α), σ_{22} and the N−H bond (β), and σ_{33} with the N−H bond (γ). Also included is the hydrogen bonding partner used in the calculations, AcAm. For clarity, all protons not involved in the hydrogen bond have been omitted.

Traceless CSA tensor was calculated by subtracting the isotropic value from each eigenvalue of the shielding tensor. This was done to allow direct comparison to average experimental values obtained previously for ubiquitin that was aligned in a liquid crystal medium.[16] In addition, the antisymmetric tensor was also analyzed to determine its possible contribution to H^N relaxation rates (vide infra).

All computations were carried out in a parallel fashion using four processors on a Silicon Graphics R12000 workstation with 2 Gb of internal memory. Computation times varied greatly depending on the type and number of atoms involved in the calculation. Using arginine residues as a benchmark, structure optimization using the 6-311**G basis set took 10 h to converge, on average. The optimized structure was used as input for the shielding calculations using the 6-311++G basis set which took 12 h to complete, whereas calculations using the 6-311++G(2d,2p) basis set took 20 h to complete on average for a given arginine residue. These values represent the longest computation time of any residue in our study. The shortest compute times involved the glycine residues, with averages of 3 h for the 6-311++G basis set, 4 h for the 6-311++G(2d,2p) basis set, and 3 h for optimization using the 6-311**G basis set. All optimizations were done at the Hartree-Fock level of theory, while shielding calculations were carried out using DFT level of theory with the B3LYP option in Gaussian.

Results

Basis Set Dependence of DFT Calculations. Three basis sets were used in the shielding tensor calculation, 6-311**G, 6-311++G, and 6-311++G(2d,2p). The best fit between experimental[10] and ab initio calculated values for σ_{iso} and $\sigma_{||}-\sigma_{\perp}$ was obtained for the 6-311++G(2d,2p) basis set, resulting

(13) Wu, C. H.; Ramamoorthy, A.; Gierasch, L. M.; Opella, S. J. *J. Am. Chem. Soc.* **1995**, *117*, 6148−6149.
(14) Gu, Z. T. T.; Opella, S. J. *J. Magn. Reson.* **1999**, *140*, 340−346.
(15) Gerald, R.; Bernhard, T.; Haeberlen, U.; Rendell, J.; Opella, S. J. *J. Am. Chem. Soc.* **1993**, *115*, 777−782.
(16) Cornilescu, G.; Bax, A. *J. Am. Chem. Soc.* **2000**, *122*, 10143−10154.
(17) Vijay-Kumar, S.; Bugg, C. E.; Cook, W. J. *J. Mol. Biol.* **1987**, *194*, 531−544.
(18) Brunger, A. T. *XPLOR Manual Version 3.1*; Yale University: New Haven, Connecticut, 1993.
(19) Sitkoff, D.; Case, D. A. *Prog. Nucl. Magn. Reson. Spectrosc.* **1998**, *32*, 165−190.
(20) Woolf, T. B.; Malkin, V. G.; Malkina, O. L.; Salahub, D. R.; Roux, B. *Chem. Phys. Lett.* **1995**, *239*, 186−194.

Table 1

		6-311**G[a] (ppm)	r^b	6-311++G[a] (ppm)	r^b	6-311++G(2d,2p)[a] (ppm)	r^b	experimental[c] (ppm)
[a]sheet (19)	σ_{iso}	41.5 (22.0)	0.22	25.9 (3.8)	0.34	23.6 (1.2)	0.91	8.7 (0.6)
	$\sigma_{\|\|}-\sigma_\perp$	12.4 (5.7)	0.42	15.6 (1.9)	0.79	11.3 (2.1)	0.71	10.6 (2.0)
helix (12)	σ_{iso}	29.5 (12.6)	0.08	31.1 (11.2)	0.66	24.8 (0.9)	0.59	8.1 (0.5)
	$\sigma_{\|\|}-\sigma_\perp$	11.7 (2.2)	0.57	12.4 (2.1)	0.75	8.3 (2.0)	0.58	6.9 (1.4)
all (36)	σ_{iso}	35.3 (18.5)	0.04	28.2 (7.7)	0.29	24.3 (1.3)	0.87	8.4 (0.6)
	$\sigma_{\|\|}-\sigma_\perp$	12.5 (4.6)	0.38	14.5 (2.7)	0.78	10.3 (2.8)	0.77	9.2 (2.5)

[a] Basis set dependence of average H^N chemical shielding values. Averages were taken over all residues participating in a particular secondary structure (number in parentheses). Standard deviations are given in parentheses. Helix includes α and 3^{10} helices. [b] Correlation factor (r) between calculated and experimental values. [c] Experimental values taken from solution NMR study.[1]

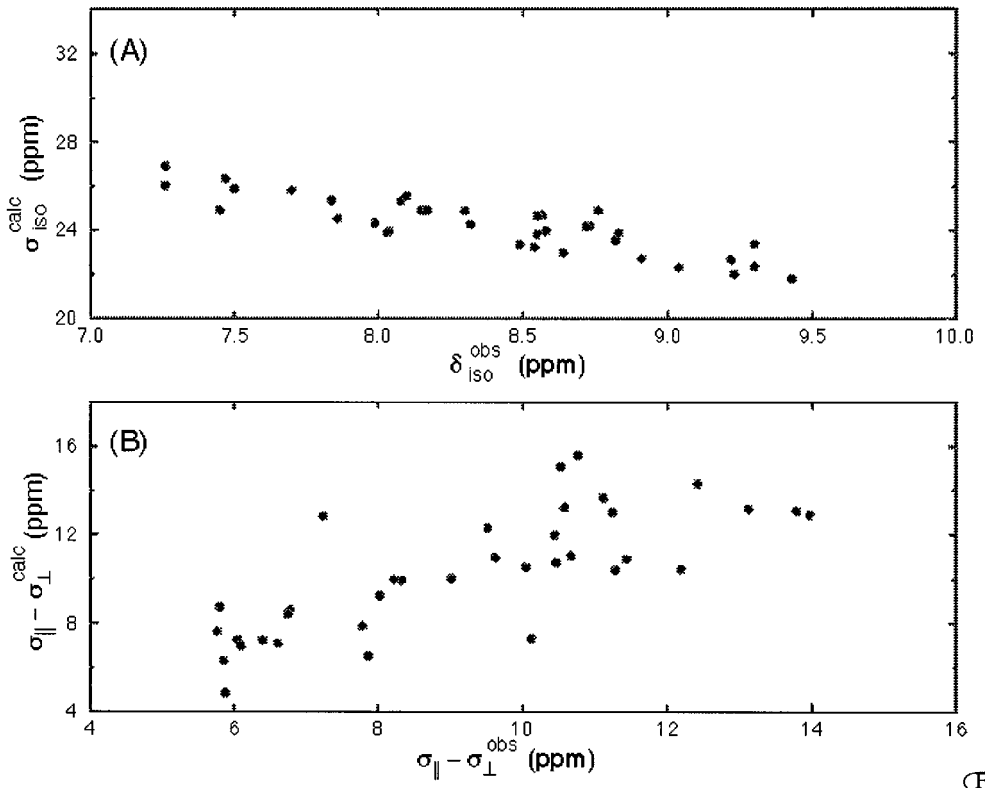

Figure 2. Comparison of calculated isotropic shielding and experimentally determined isotropic chemical shift values (A) for nonsolvent exposed 36 residues in human ubiquitin. Calculations were done with the 6-311++G(2d,2p) basis set. A reasonably good correlation is indicated by a high ($r = 0.87$) correlation factor. Similar comparison for the $\sigma_{\|}-\sigma_\perp$ values (B) shows a slightly worse correlation with a correlation factor of 0.77.

in correlation coefficients $r_{iso} = 0.87$ and $r_{ani} = 0.77$ for σ_{iso} and $\sigma_{\|}-\sigma_\perp$, respectively. Table 1 lists the basis set dependence of σ_{iso} and $\sigma_{\|}-\sigma_\perp$ (average values) with respect to the secondary structure, along with correlation to experimentally determined chemical shift values. It is important to note that the 6-311++G basis set yields a value for r_{ani} (0.78) close to that seen with 6-311++G(2d,2p) ($r_{ani} = 0.77$), but a much lower value for r_{iso} (0.29 versus 0.87). The lower r_{iso} value for the 6-311++G basis set is due to four outliers (E34, R42, R54, Y59), with σ_{iso} values between 40 and 60 ppm. The optimization of these residues failed to converge properly leading to the poor agreement in their calculated shielding to the experimentally observed ones. Excluding these outliers in calculating the correlation factor results in $r_{iso} = 0.84$, similar to the value using the 6-311++G(2d, 2p) basis set ($r_{iso} = 0.87$). We will bear this in mind in the subsequent analysis.

Correlation between Experimental and Calculated Shielding Values. The average calculated principal values are 18.1 ± 2.1, 23.0 ± 1.9, and 31.7 ± 1.1 ppm for σ_{11}, σ_{22}, and σ_{33}, respectively, while the average calculated angles that the principal vector make with the N−H bond are 93.7 ± 9.0°, 84.9 ± 8.8°, and 12.3 ± 6.6° for σ_{11}, σ_{22}, and σ_{33}, respectively. The σ_{11} axis is orthogonal to the peptide plane, the σ_{22} axis is perpendicular to the N−H bond and in the peptide plane, and σ_{33} is almost parallel to the N−H bond. Figure 2A and B shows the correlation between the experimental and calculated values for the 6-311++G(2d,2p) basis set. The correlation is found to be much better for the isotropic than the anisotropic values. Note that the calculated isotropic shielding values are compared to the experimental shift values. Similar calculations on a reference compound which would permit the conversion of shielding to shift values were not performed as our calculations were very computationally expensive.

The slope seen in the anisotropic case is close to one (Figure 2B) using this dense basis set. The smaller 6-311++G basis set also gave a similar slope (0.86) and correlation ($r_{ani} = 0.78$) to this basis set. However, the smaller basis set tended to overestimate the experimental values by an average of 5.3 ± 1.7 ppm. Repeating the calculations with the larger basis set reduced the offset to 1.1 ± 1.8 ppm. The use of the larger basis

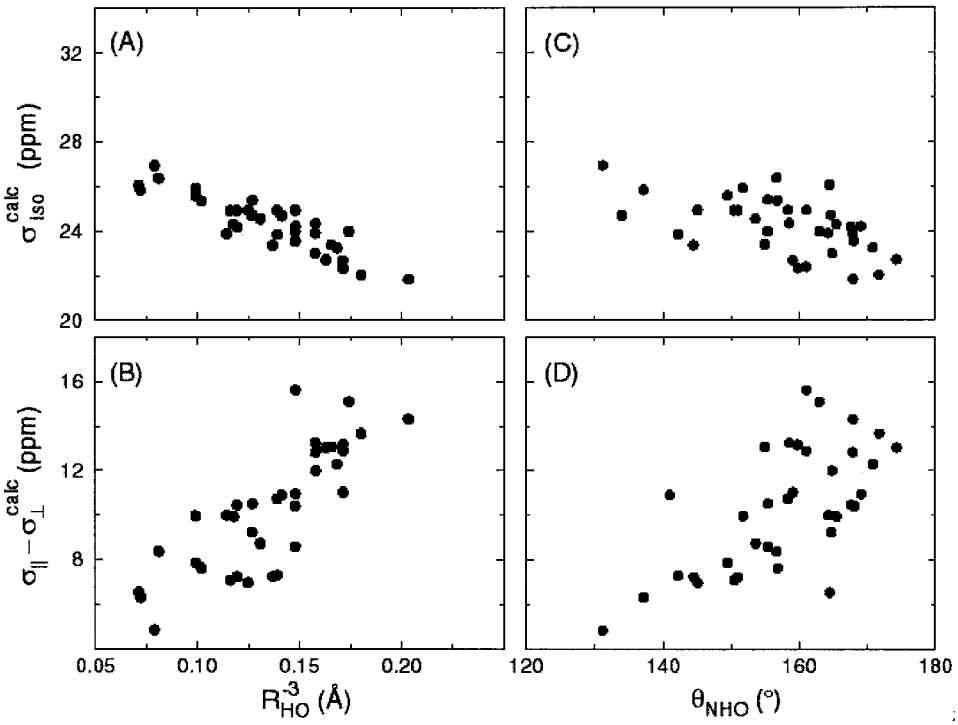

Figure 3. Correlation between hydrogen bond length (R_{HO}) and calculated σ_{iso} and $\sigma_{||}-\sigma_{\perp}$ values (A,B) as well as correlation between hydrogen bond angle (θ_{NHO}) and σ_{iso} and $\sigma_{||}-\sigma_{\perp}$ (C,D). Better correlation can be observed for σ_{iso} and $\sigma_{||}-\sigma_{\perp}$ to the hydrogen bond length ($r = 0.86$ and $r = 0.78$, respectively) as compared to the hydrogen bond angle ($r = 0.54$ and $r = 0.63$, respectively).

set, while not improving slope or correlation, yielded $\sigma_{||}-\sigma_{\perp}$ values closer to those observed in the experiment. The good correlations with the experimental data validate our ab initio shielding calculation protocol. This serves as a starting point for us to explore, in greater detail, factors contributing to shielding, such as hydrogen bond length and angle, as well as backbone dihedral angle, in an effort to provide insight into the relationship between local structure and chemical shielding.

Dependence of Shielding on Hydrogen Bond Length. The correlation between H^N CSA in ubiquitin and hydrogen bond strength has been previously demonstrated experimentally.[10] In addition, an isotropic chemical shift has also been shown to be an indicator of hydrogen bond strength.[5,21−23] Indeed, we have also observed a correlation between σ_{iso}, $\sigma_{||}-\sigma_{\perp}$, and hydrogen bond length (R_{HO}) and angle (θ_{NHO}). Figure 3 shows the variation in σ_{iso} and $\sigma_{||}-\sigma_{\perp}$ as a function of $1/R^3_{HO}$ (A,B) and θ_{NHO} (C,D). Hydrogen bond length correlates well with σ_{iso}, with a correlation coefficient of $r_{iso} = 0.89$, and also with $\sigma_{||}-\sigma_{\perp}$, yielding $r_{ani} = 0.81$. Slightly lower correlation coefficients of $r_{iso} = 0.88$ and $r_{ani} = 0.80$ were obtained for σ_{iso} and $\sigma_{||}-\sigma_{\perp}$, respectively, as a function of $1/R_{HO}$. This is in agreement with previous studies where the H^N isotropic shift is dominated by bond magnetic anisotropy that depends on the inverse third power of their distance to the amide proton.[4,24] In contrast, Wu et al. showed a clear linear dependence of the tensor components on the R_{HO}.[25] Furthermore we observe that $\sigma_{||}-\sigma_{\perp}$ increases while σ_{iso} decreases with decreasing R_{HO}. This is in agreement with solid-state[25,26] as well as solution NMR results.[10,12] The σ_{iso} values vary between 21.8 and 26.9 ppm over the range of hydrogen bond lengths studied, corresponding to a change of 23% between minimum and maximum values. In contrast, the $\sigma_{||}-\sigma_{\perp}$ values vary between 4.9 and 15.6 ppm, corresponding to more than a factor of 2 increase in range relative to the σ_{iso}. This implies that $\sigma_{||}-\sigma_{\perp}$ is much more sensitive to hydrogen bond length as compared with σ_{iso}. This behavior is clearly a result of the dependence of the individual tensor elements on R_{HO} and θ_{NHO}. We will first investigate the R_{HO} dependence of σ_{iso} and $\sigma_{||}-\sigma_{\perp}$ in more detail.

To gain further insight into how the hydrogen bond geometry influences shielding, we have plotted the principal values for individual residues as a function of R_{HO} and θ_{NHO}. Figure 4A−C shows the correlation of each diagonal component with R_{HO}. The orthogonal tensor components σ_{11} and σ_{22} show a strong correlation with positive slope, whereas σ_{33} does not show any significant correlation with R_{HO}. For the σ_{33} versus R_{HO} graph (Figure 4C), a slight tendency toward negative slope does seem evident, though the weak correlation precludes any further interpretation. On the basis of these observations, an increase in hydrogen bond strength (decreasing R_{HO}) primarily affects a decrease in the orthogonal components, σ_{11} and σ_{22}. Since the isotropic shielding depends on $^1/_3$ of the trace of the CSA tensor, this results in σ_{iso} that decreases with decreasing R_{HO}, since σ_{11}, σ_{22}, and σ_{33} are equally weighted in the calculation.

The anisotropic shielding ($\sigma_{||}-\sigma_{\perp}$), on the other hand, is dependent on the $P_2(\cos\theta)$ projection of the CSA tensor onto the N−H bond. The nature of this projection weights the contribution of σ_{33} more heavily than σ_{11} or σ_{22}, since it depends

(21) Pardi, A.; Wagner, G.; Wüthrich, K. *Eur. J. Biochem.* **1983**, *137*, 445−454.
(22) Wagner, G.; Pardi, A.; Wüthrich, K. *J. Am. Chem. Soc.* **1983**, *105*, 5948−5949.
(23) Kuntz, I. D.; Kosen, P. A.; Craig, E. C. *J. Am. Chem. Soc.* **1991**, *113*, 1406−1408.
(24) Asakura, T.; Taoka, K.; Demura, M.; Williamson, M. P. *J. Biomol. NMR* **1995**, *6*, 227−236.
(25) Wu, G.; Freure, C. J.; Verdurand, E. *J. Am. Chem. Soc.* **1998**, *120*, 13187−13193.
(26) Berglund, B.; Vaughan, R. W. *J. Chem. Phys.* **1980**, *73*, 2037−2043.

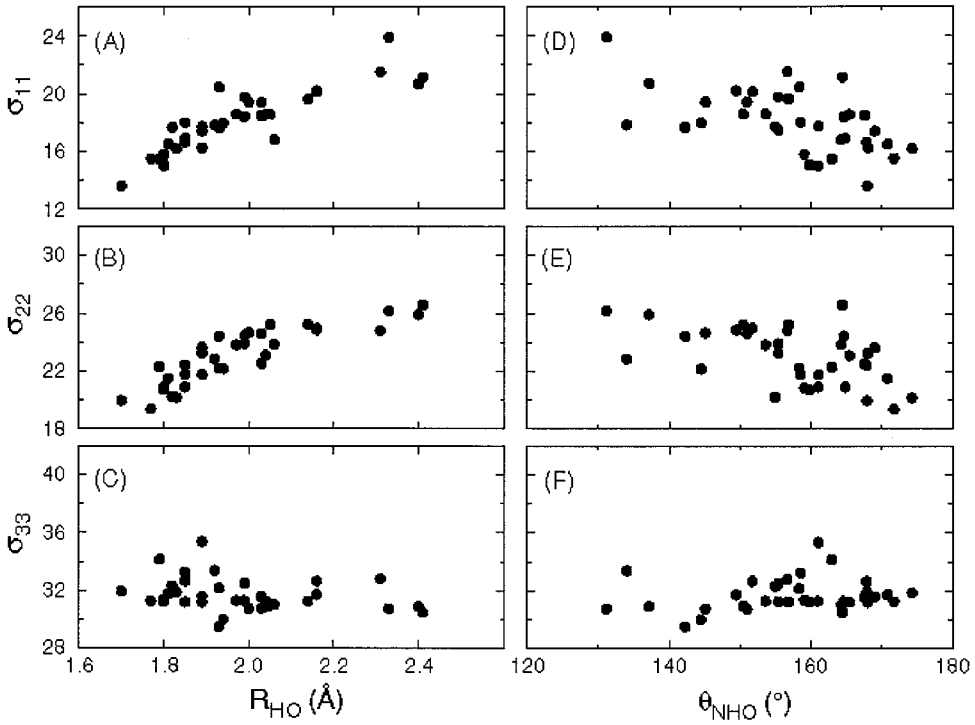

Figure 4. Correlation between principal values of the CSA tensor and hydrogen bond length, R_{HO} (A−C), and angle, θ_{NHO} (D−F). An average r value of 0.87 was calculated for σ_{11} and σ_{22} correlation to the hydrogen bond length. In contrast, significantly worse correlations were obtained for σ_{11} and σ_{22} to the hydrogen bond angle (average r value of 0.55). Almost no dependence can be observed for σ_{33} on hydrogen bond length or angle.

on the cosine of the angle made between the principal axes and the N−H bond. Since σ_{11} and σ_{22} are orthogonal to the N−H bond, they will be weighted less in the calculation. In fact, this observation may also help to explain why the calculated σ_{iso} has a better correlation to the experimental data than does $\sigma_{||}-\sigma_{\perp}$. Since σ_{33} is parallel to the N−H bond, it will be weighted more, by roughly a factor of 2, in the $\sigma_{||}-\sigma_{\perp}$ calculation. The poor correlation of R_{HO} with σ_{33} will propagate the $\sigma_{||}-\sigma_{\perp}$ calculation, affecting the overall correlation between $\sigma_{||}-\sigma_{\perp}$ and R_{HO}. In the case of σ_{iso}, the σ_{11}, σ_{22}, and σ_{33} values are equally weighted. Therefore σ_{33} contributes less in the calculation, resulting in a better overall correlation for σ_{iso} than for $\sigma_{||}-\sigma_{\perp}$.

Dependence of Shielding on Hydrogen Bond Angle. Since not only hydrogen bond distance between donor and acceptor but also the angle between them[27] affects its strength, the variation in chemical shielding was also investigated as a function of the hydrogen bond angle, θ_{NHO} (Figure 3C and D). The correlation between θ_{NHO} and shielding is much less than seen with R_{HO} (Figure 3A and B), implying that the angle plays less of a role in determining σ_{iso} and $\sigma_{||}-\sigma_{\perp}$ than does R_{HO}. Since all calculations were carried out on geometry derived from the X-ray structure, the imprecision in determining the exact hydrogen bond angle from the X-ray structure will introduce scatter in all of these correlation plots equally. We also see similar behavior with respect to hydrogen bond strength as seen with R_{HO}. As θ_{NHO} approaches 180°, hydrogen bonding strength approaches a maximum. Figure 3C and D shows that as θ_{NHO} approaches 180°, σ_{iso} decreases, whereas $\sigma_{||}-\sigma_{\perp}$ increases. Thus σ_{iso} decreases as hydrogen bond strength increases, whereas $\sigma_{||}-\sigma_{\perp}$ increases. We also see similar behavior for the individual tensor elements (Figure 4D−F). The tensor components σ_{11} and σ_{22} decrease with increasing θ_{NHO}, and σ_{33} shows little correlation with θ_{NHO}. However, the correlations in this case are too low to justify further analysis, thus prompting the need for an analysis where the effects of θ_{NHO} and R_{HO} can be isolated.

Single Residue Study of R_{HO} and θ_{NHO}. To gauge the influence of R_{HO} and θ_{NHO} on the CSA tensor independent of effects from residue differences, we calculated σ_{iso} and $\sigma_{||}-\sigma_{\perp}$ for a single residue (A28), while independently incrementing R_{HO} and θ_{NHO}. The calculations were performed on A28 hydrogen bonded to AcAm, using the 6-311++G basis set. It was noted previously that this basis set yielded similar results to 6-311++G(2d,2p) once the four outliers were removed (E34, R42, R54, Y59). We justify the use of this smaller basis set by noting that this basis set provides similar correlation to the experimental data (provided the four outliers are removed) as does 6-311++G(2d,2p). In addition, we are only concerned with the relative variations of σ_{iso} and $\sigma_{||}-\sigma_{\perp}$ with respect to R_{HO} and θ_{NHO} and not the absolute magnitudes. Once the hydrogen bond geometry was modified, the structure was reoptimized without constraining the hydrogen bond to check for a possible energetically unfavorable conformation. Varying the hydrogen bond distance while keeping the angle fixed, or vice versa, did not seem to have any consequences on the overall quality of the geometry.

Figure 5 shows σ_{iso} and $\sigma_{||}-\sigma_{\perp}$ as a function of hydrogen bond strength. We see the same behavior as in the previous case, namely σ_{iso} decreases with increasing hydrogen bond strength, whereas $\sigma_{||}-\sigma_{\perp}$ increases. It is also apparent from these data that $\sigma_{||}-\sigma_{\perp}$ is more sensitive to changes in R_{HO} or θ_{NHO} than is σ_{iso}. In fact, Figure 5C shows that σ_{iso} changes relatively little over the range of angles studied. On the other hand, $\sigma_{||}-\sigma_{\perp}$ changes ~13 ppm over the same range, indicating the

(27) Kabsch, W.; Sander, C. *Biopolymers* **1983**, *22*, 2577−2637.

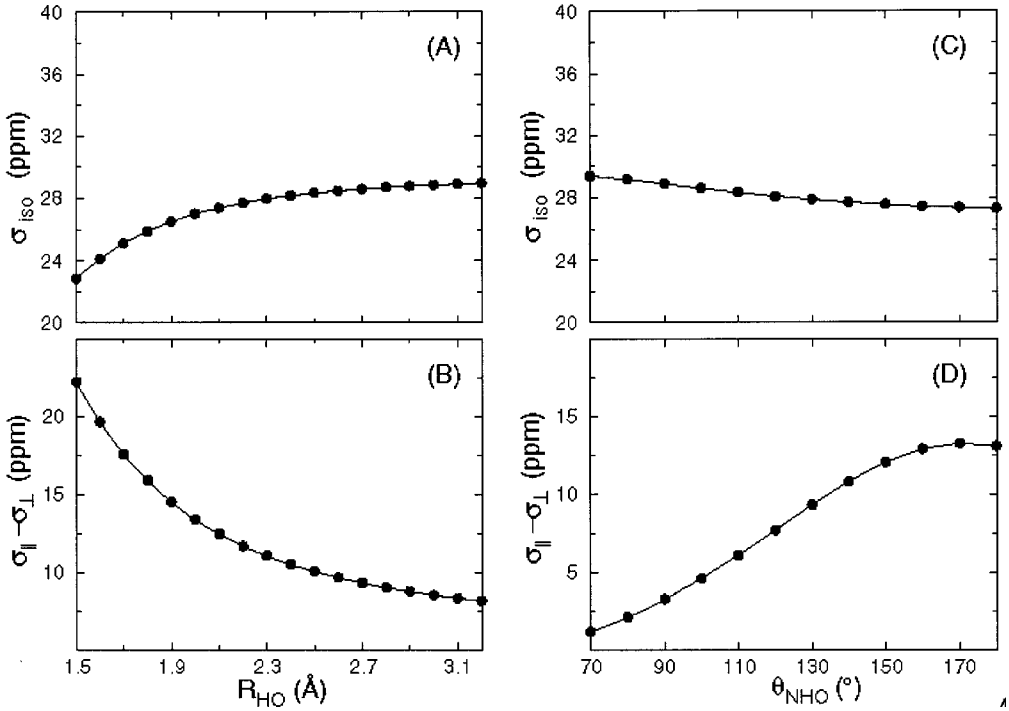

Figure 5. Change in σ_{iso} and $\sigma_{||}-\sigma_{\perp}$ (in ppm) as a function of R_{HO} (A,B) and θ_{NHO} (C,D) for the A28−AcAm complex. The $\sigma_{||}-\sigma_{\perp}$ shows at least a factor of 2 larger change as a function of R_{HO} relative to the σ_{iso}, while $\sigma_{||}-\sigma_{\perp}$ is a factor of 5 more sensitive to changes in θ_{NHO} as compared to σ_{iso}.

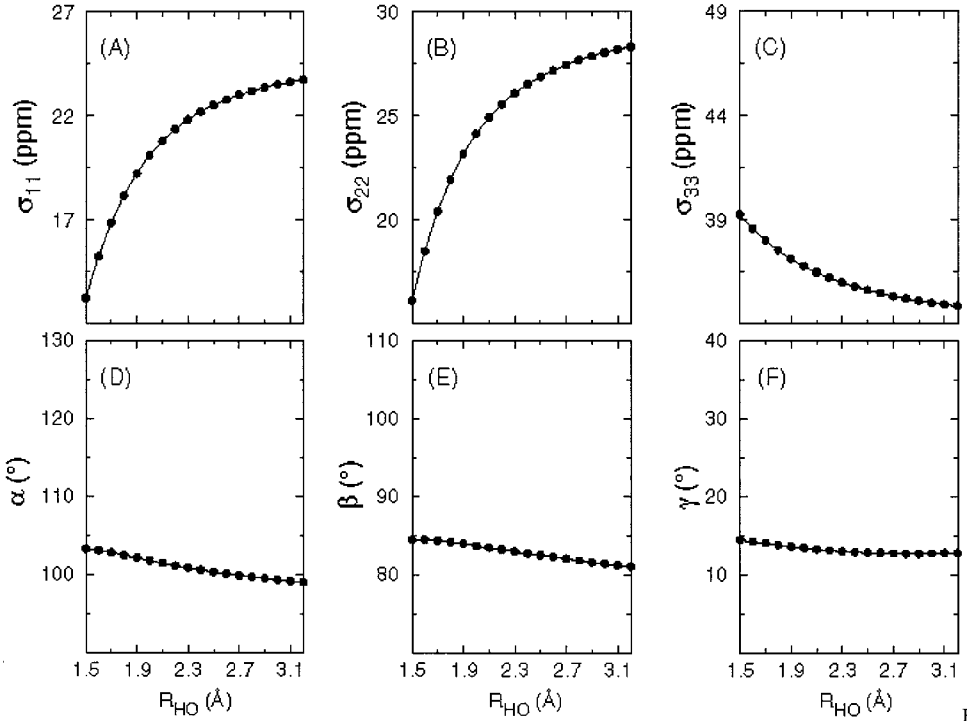

Figure 6. Principal values (A−C) and orientation of the CSA tensor (D−F) as a function of R_{HO} for the A28−AcAm complex. Orientations are defined as the angle made between σ_{11} and the N−H bond (α), σ_{22} and the N−H bond (β), and σ_{33} with the N−H bond (γ).

sensitivity of this parameter to the hydrogen bond angle. However, $\sigma_{||}-\sigma_{\perp}$ seems to vary slightly more with R_{HO} than with θ_{NHO}. These data may imply that $\sigma_{||}-\sigma_{\perp}$ is a more sensitive gauge of changes in local structure than is σ_{iso}. To investigate this more rigorously, we will analyze the individual tensor components and angles as a function of hydrogen bond strength.

Based on Figures 6 and 7, in general, H^N shielding is more sensitive to R_{HO} than to θ_{NHO}. The principal values σ_{11}, σ_{22}, and σ_{33} vary to a larger degree as a function of R_{HO}, depicted in Figure 6A−C. The orientation of the principal values as a function of R_{HO} and θ_{NHO} is also indicated. The tensor orientation (α, β, γ) appears to be significantly dependent on θ_{NHO}. In contrast, R_{HO} appears to have only a slight effect on tensor orientation. This implies that tensor orientation is not a key factor in determining the contribution of the tensor components to either σ_{iso} or $\sigma_{||}-\sigma_{\perp}$ as a function of R_{HO}.

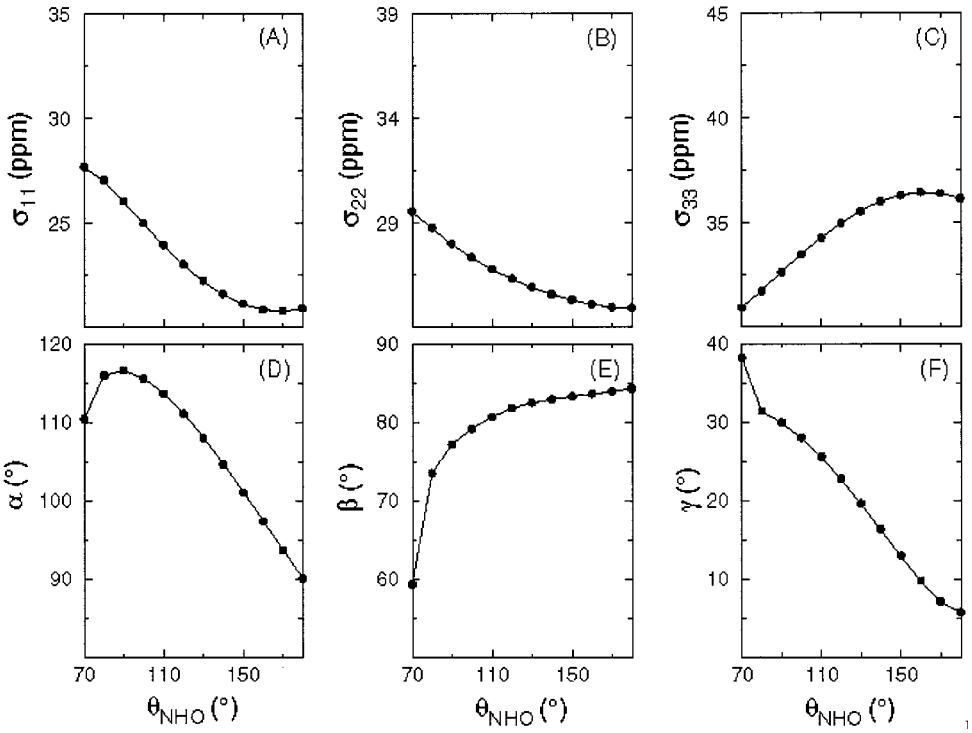

Figure 7. Principal values (A−C) and orientation of the CSA tensor (D−F) as a function of θ_{NHO} for the A28−AcAm complex. Orientations are defined as the angle made between σ_{11} and the N−H bond (α), σ_{22} and the N−H bond (β), and σ_{33} with the N−H bond (γ).

However, we see that for θ_{NHO} the behavior of the principal values generally agrees with what is expected. For example, as γ approaches 0°, σ_{33} increases. This is consistent with maximum shielding occurring when γ is almost parallel to the N−H bond. Furthermore as β increases, σ_{22} decreases, while as α decreases, σ_{11} also decreases. This suggests that the dependence of the principal values on the hydrogen bond angle may result from a reorientation of the CSA tensor. A slight reorientation of the principal axes as a function of R_{HO} can be observed; however, this amounts to a maximum change of roughly 4°, and it is not expected to contribute significantly to the $\sigma_{||}-\sigma_{\perp}$ or σ_{iso} values. However, other effects from R_{HO} obviously play a large role in the determination of these parameters, as the principal values vary greatly as a function of R_{HO}. This appears to explain why σ_{iso} varies little, while $\sigma_{||}-\sigma_{\perp}$ varies to a far greater extent. The anticorrelated behavior of σ_{11} and σ_{22} versus σ_{33} will tend to minimize the effects when taking the average of these three values, whereas the $\sigma_{||}-\sigma_{\perp}$ calculation will tend to emphasize the value of σ_{33} (since it is weighted heavily in the calculation, being almost parallel to the N−H bond). All of these combined implies that $\sigma_{||}-\sigma_{\perp}$ is a better indicator of hydrogen bond length and angle than is σ_{iso}.

Variation in $\sigma_{||}-\sigma_{\perp}$ and σ_{iso} for Different Residues with Fixed θ_{NHO} and R_{HO}. To address the possible contribution from the secondary structure (or the φ and ψ dihedral angles) as well as amino acid type to H^N shielding, we fixed the values at the average for the 36 residues studied (R_{HO} = 2.0 Å, θ_{NHO} = 157.6°) and recalculated σ_{iso} and $\sigma_{||}-\sigma_{\perp}$. Eleven residues were chosen (five β-sheet, five α-helix, one β-turn) which span different types of secondary structure. Table 2 lists the residues, along with the corresponding shielding, principal values and the φ as well as ψ dihedral angles. Shielding values listed in Table 2 clearly show a small dependence of shielding on the secondary structure or φ and ψ dihedral angles. On average, helical residues have a $\sigma_{||}-\sigma_{\perp}$ value that is lower by about 0.5 ppm and a σ_{iso} value that is higher by 0.9 ppm than those in the β-sheet. However, residue in a turn seems to have a $\sigma_{||}-\sigma_{\perp}$ value that resembles a β-sheet residue, while its σ_{iso} value is close to a helical residue. The variations in φ and ψ dihedral angles seem to affect all principal components of the tensor equally. These calculations also show no clear or perhaps a very weak dependence of shielding on amino acid type. This is consistent with the H^N random coil shifts that cover a maximum range of 0.6 ppm[1] that would be very hard to distinguish from a similarly weak effect due to the backbone φ and ψ dihedral angles.

Table 2

2° struct	residue	$\sigma_{||}-\sigma_{\perp}$ (ppm)	σ_{iso} (ppm)	σ_{11} (ppm)	σ_{22} (ppm)	σ_{33} (ppm)	ϕ^b	ψ^b
[a]sheet	F4	10.6	23.5	17.9	21.7	30.8	−116.0	140.2
	V5	10.8	23.4	16.8	22.4	30.9	−118.0	114.2
	T7	10.1	24.8	18.2	24.3	31.8	−99.6	170.8
	I13	9.9	23.6	17.0	22.6	31.4	−109.5	142.0
	V17	10.3	23.4	17.6	20.9	31.7	−139.0	170.7
helix	V26	9.6	24.4	18.0	23.6	31.6	−58.4	−46.4
	K27	9.5	24.6	18.0	24.1	31.5	−60.8	−38.0
	A28	10.3	24.5	18.3	23.1	32.0	−66.1	−38.1
	K29	9.5	24.3	18.2	23.5	31.3	−64.2	−37.3
	E34	10.7	25.0	20.5	22.4	32.2	−123.6	−6.4
turn	D21	10.8	24.3	17.2	23.9	31.7	−71.0	148.4

[a] Variation in σ_{iso} and $\sigma_{||}-\sigma_{\perp}$ with fixed R_{HO} and θ_{NHO} values. [b] Backbone dihedral angles were taken from X-ray coordinates.[17]

Contribution from the Antisymmetric Tensor (T^A) on Relaxation. The antisymmetric portion of the chemical shielding tensor **T** (T^A) has been shown previously to potentially contribute to nuclear spin relaxation for ^{15}N.[28,29] We wish to

(28) Kowaleski, J.; Werbelow, L. *J. Magn. Reson.* **1997**, *128*, 144−148.
(29) Scheurer, C.; Skrynnikov, N. R.; Lienin, S. F.; Strauss, S. K.; Bruschweiler, R.; Ernst, R. R. *J. Am. Chem. Soc.* **1999**, *121*, 4242−4251.

Table 3

	traceless symmetric ($\mathbf{T}^S$)				antisymmetric ($\mathbf{T}^A$)		
res used	σ_{11} (ppm)	σ_{22} (ppm)	σ_{33} (ppm)	η	σ_{12} (ppm)	σ_{13} (ppm)	σ_{23} (ppm)
all (36)	−6.2 (1.1)	−1.2 (1.0)	7.4 (1.6)	0.67 (10.2)	0.3 (0.3)	−0.1 (0.5)	0.1 (0.4)
helix (12)	−5.6 (1.1)	−0.8 (0.8)	6.4 (1.2)	0.75 (0.2)	0.4 (0.4)	0.04 (0.3)	0.3 (0.3)
sheet (19)	−6.5 (0.8)	−1.4 (1.0)	7.9 (1.3)	0.64 (0.2)	0.2 (0.3)	−0.2 (0.4)	0.2 (0.4)

[a] Averages over all residues participating in a particular secondary structure (number of residues used in the average given in parentheses). Helix includes the α and 3^{10} helices. Standard deviations are given in parentheses. The asymmetry (η) values were determined using the definition published previously.[16]

investigate this possibility for our current study on H^N tensors. To take into account the possible effect of the antisymmetric tensor on the longitudinal or transverse relaxation rates, one can write its contribution to spectral densities, considering the simplest case of isotropic reorientation, as[28,30]

$$J_s(\omega) = \frac{{\omega_0}^2\tau_c}{60(1+{\omega_0}^2{\tau_c}^2)}[(\sigma_{11}-\sigma_{22})^2+(\sigma_{11}-\sigma_{33})^2+(\sigma_{22}-\sigma_{33})^2] \quad (1)$$

$$J_a(\omega) = \frac{{\omega_0}^2\tau_c}{8(1+9{\omega_0}^2{\tau_c}^2)}[(\sigma_{12}-\sigma_{21})^2+(\sigma_{13}-\sigma_{31})^2+(\sigma_{23}-\sigma_{32})^2] \quad (2)$$

where τ_c is the reorientational correlation time, and ω_0 is the Larmor frequency. $J_s(\omega)$ and $J_a(\omega)$ represent spectral densities contributions from the symmetric and antisymmetric CSA tensor, respectively. As is characteristic of antisymmetric tensors, the diagonal elements vanish, and the off diagonal elements are related as $\sigma_{12} = -\sigma_{21}$, $\sigma_{13} = -\sigma_{31}$, $\sigma_{23} = -\sigma_{32}$; therefore, only three tensor elements are needed to define the matrix. Table 3 lists the diagonal tensor elements and the asymmetry (η) for the traceless symmetric tensor as well as relevant elements for the antisymmetric tensor.

To quantify the contribution of $\mathbf{T}^A$ to the relaxation rates, we calculated $(R_i)_a/R_i$ (i = 1,2) as a function of $\omega_0\tau_c$ for the average values listed in Table 3, in a fashion similar to the aforementioned study.[28] The contribution from the antisymmetric tensor is highest in the fast tumbling limit ($\omega_0\tau_c \ll 1$). For the helix average, the antisymmetric tensor results in a maximum contribution to the relaxation rates of 3.5% and 1.5% for R_1 and R_2, respectively. When including all 36 residues, the contribution drops to 1.1% and 0.5% for R_1 and R_2, respectively. The β-sheet residues have a maximum contribution of 0.7% and 0.3% for R_1 and R_2, respectively. We refrain from making conclusions based on differences in the helix, sheet, and all of the residues averages, as the standard deviations in them are too high to make quantitative comparisons. However, on the basis of these calculations, we see the maximum contribution to relaxation rates from the antisymmetric tensor is not greater that 3.5% for R_1 and 1.5% for R_2 and therefore is not expected to play a significant role in the calculation of relaxation rates in the limit of isotropic reorientation.

Discussion

Our result represents the first extensive attempt in decomposing various structural contributions to H^N shielding. Earlier published experimental results provided a valuable evaluation for our ab initio calculation protocol.[10,16] The requirement for a very high basis set to obtain an accurate shielding tensor was apparent in the results of our calculations. A minimum of a 6-311++G basis set is needed to reproduce the tendencies of the experimental anisotropic shielding values. A higher 6-311++G(2d,2p) basis set would be preferable if computational time was not limited. The calculated tensor component is the largest along the N−H bond (σ_{33}), followed by the smaller σ_{22} that is nearly perpendicular to the N−H bond and close to being in the peptide plane and the smallest σ_{11} which is orthogonal to the peptide plane. The calculated tensor is far from being axially symmetric, which is in agreement with previous solution NMR experimental results.[16] However, small errors of the smallest component (σ_{22}) produce an uncharacteristically large standard of deviation prohibiting the determination of the asymmetry parameter accurately. The calculated antisymmetric tensor components are consistently small, thus safely allowing their omission from consideration in relaxation studies.

The H^N tensor shows no clear dependence on amino acid type. While it does seem to have a weak dependence on secondary structure, the tensor is primarily affected by hydrogen bond strength. Interestingly, hydrogen bonding affects the tensor element that is close to being parallel to it (σ_{33}) the least. Large changes in the magnitude of the tensor components perpendicular to the hydrogen bond (σ_{11} and σ_{22}) were observed as a function of hydrogen bond length. They become less shielded as the hydrogen bond distance decreases. This result is consistent with a previous study of the hydrogen bond effect on proton chemical shift in crystalline hydrates.[25] Almost no variations in the tensor direction could be observed as a function of hydrogen bond length. The total change was roughly 11, 12, and 4 ppm for the σ_{11}, σ_{22}, and σ_{33}, respectively, over the range of hydrogen bond lengths calculated. However, the dependence of σ_{33} is reversed to that of the other two elements, with decreasing magnitude as hydrogen bond distance increases. This clearly desensitizes the isotropic shielding, while it increases the sensitivity by greater than a factor of 2 of the anisotropic shielding on hydrogen bond distance. This result confirms earlier experimental findings.[10]

In addition to the hydrogen bond length, the tensor also depends on the hydrogen bond angle. So far earlier experimental results from solution NMR could not address this factor. Our calculation suggests that the largest change of 7, 5, and 5 ppm can be observed for the σ_{11}, σ_{22}, and σ_{33}, respectively, over hydrogen bond angles from 180° (parallel) to 70°. This leads to a maximum change in $\sigma_{||}-\sigma_{\perp}$ of 12 ppm over the same range of angles. In contrast, due to the reversed dependence of σ_{33} on the hydrogen bond angle relative to the other two components, the isotropic value only changes by a maximum of 3 ppm. In

(30) Blicharski, J. S. *Z. Naturforsch., A: Phys. Sci.* **1972**, *27*, 1456.

addition, the tensor direction could change by as much as 30° as a function of the hydrogen bond angle. The orientation of the tensor component σ_{33}, which is almost parallel to the hydrogen bond, tends to follow the hydrogen bond angle. Furthermore, the asymmetry of the tensor seems to have a weak dependence on the hydrogen bond angle as well (data not shown). This is in agreement with the finding of Wu et al.[25] Obviously smaller ranges will be expected if one limits the typical acceptable hydrogen bond angles to a minimum of 120°.

A ^{15}N solid-state NMR study of polypeptides has been carried out to try to elucidate the ^{15}N shielding tensor dependence on the hydrogen bond as well as the primary, secondary, and higher ordered structure of polypeptides.[31] Unlike the amide proton shielding tensor, the amide nitrogen tensor is quite sensitive to the primary structure or amino acid sequence as well as the secondary structure of the polypeptide. Furthermore, the amide ^{15}N tensor component that is the most sensitive to the hydrogen bond geometry (σ_{11}) is the one that is almost parallel to it. This is exactly opposite of the amide proton case. In addition, the σ_{33} of the amide ^{15}N tensor is related to the side-chain structures of the polypeptide. In the case of the amide proton, no clear conclusion with respect to the side chain can be derived from our study so far. However, our results suggest that this contribution most likely will be small.

Asakura et al. carried out an empirical study of amide proton isotropic chemical shift using available data from high-resolution X-ray structures of 15 proteins.[24] In this study, the H^N shielding is considered as a sum of several effects: ring current effect, magnetic anisotropy effect from the carbonyl and C−N bonds of amide groups, and electric field effect. These effects were calculated on the basis of the geometry of the relevant chemical groups obtained from the X-ray structures. An empirical set of parameters was then obtained from fitting the calculated chemical shifts to the corresponding values in the database. Several conclusions can then be derived from the fitted parameters. For instance, the electrical field contribution was found to be negligible for the H^N shift. Furthermore, the magnetic anisotropy of the carbonyl group of the hydrogen bond acceptor was found to be the dominant term. Upfield H^N shift for helices and the downfield trend observed for the β-sheet are well known.[5,8,32−35] Asakura et al. attributed this to the overall upfield shift in helices due to the long-range effect originating in residues i-2 and i-3.[24] Our calculations inherently take into account these effects. However, the long-range nature of our calculations is limited to the chemical moiety included in the calculations, which typically is dictated by the limited computational time. However, from the good agreement that we observed with the measured isotropic and anisotropic chemical shifts, we can conclude that if the bond magnetic anisotropy was the important effect then the dominant term would come from the carbonyl group of the hydrogen bond acceptor. In this respect, our result is in agreement with Asakura et al. On the other hand, on the basis of the same observation, we can conclude that the upfield shift observed in helices is not entirely due to the long-range effect of the bond magnetic anisotropy. In fact it is the typical length of the hydrogen bond found in the two secondary structures that dictates the H^N shift with a small contribution coming from the dihedral angle dependence. Another possible long-range effect is ring current. In ubiquitin this effect on H^N shift is minimal due to the total number of the aromatic groups in the protein as well as their proximity to the H^N of the residues used in our calculations. Note that in our calculations no assumptions were made other than the adequacy of our basis set. In contrast, other studies involving chemical shift from a database have to assume that changes due to variations in sample conditions such as temperature, salt concentration, and pH can be taken into account properly.

Our calculations have clearly illustrated a feasible approach in separating various contributions to the H^N shielding tensor. The largest contribution is the hydrogen bond strength. This conclusion cannot be achieved unequivocally with experimental data alone. Considering the wealth of structural information that shielding tensors typically contain, their values are definitely underutilized in structure determination. Studies similar to the one presented here will bring us closer to a better understanding of various aspects of shielding tensors, thus allowing their practical use in structure determination.

JA016859D

(31) Shoji, A.; Ozaki, T.; Fujito, T.; Deguchi, K.; Ando, S.; Ando, I. *J. Am. Chem. Soc.* **1990**, *112*, 4693−4697.
(32) Markley, J. L.; Meadows, D. H.; Jardetzky, O. *J. Mol. Biol.* **1967**, *27*, 25−40.
(33) Clayden, N. J.; Williams, R. J. P. *J. Magn. Reson.* **1982**, *49*, 383−396.
(34) Dalgarno, D. C.; Levine, B. A.; Williams, R. J. P. *Biosci. Rep.* **1983**, *3*, 443−452.
(35) Szilágyi, L.; Jardetzky, O. *J. Magn. Reson.* **1989**, *83*, 441−449.